Assessing and Mapping the Flood Vulnerability of Krueng Baro Watershed, Aceh, Indonesia Using GIS-Based Hierarchical Criteria Analysis

Rahmi Rahmi
Doctoral Program of Engineering, Postgraduate School, Universitas Syiah Kuala, Banda Aceh, Aceh, Indonesia
rahmi_hd@yahoo.com

Ashfa Achmad
Architecture and Planning Department, Universitas Syiah Kuala, Banda Aceh, Aceh, Indonesia
ashfa.achmad@usk.ac.id (corresponding author)

Alfiansyah Yulianur
Civil Engineering Department, Universitas Syiah Kuala, Banda Aceh, Aceh, Indonesia
fian_7anur@usk.ac.id

Ichwana Ramli
Agricultural Engineering Department, Universitas Syiah Kuala, Banda Aceh, Aceh, Indonesia
ichwana.ramli@usk.ac.id

Received: 3 December 2025 | Revised: 15 January 2026 | Accepted: 27 January 2026

 DOI: https://doi.org/10.48084/etasr.16368

ABSTRACT

Land Use and Land Cover (LULC) change has increasingly shaped flood vulnerability across many watersheds, including those in Indonesia. In the Krueng Baro Watershed in Aceh, the rapid conversion of permeable areas into impervious surfaces has reduced infiltration capacity, increased runoff, and intensified river discharge, thereby expanding flood-prone zones. This study aims to map and evaluate flood vulnerability by adopting an approach that accounts for greater variation in several biophysical parameters. A scoring and weighting approach was applied using 2019 LULC data and six variables: rainfall, soil type, slope gradient, river density, land use, and elevation. To strengthen the analysis, additional simulations were conducted with different variable combinations to assess model sensitivity. The results indicate that river density, elevation, and land use exert the strongest influence, with high river density, low elevation, and intensive land use closely associated with deeper and more extensive flooding. These findings underscore the urgent need for spatial planning and environmental management strategies, particularly through ecosystem restoration, periodic land-use planning reviews, and river normalization. Beyond providing technical insights, this study offers a practical framework that is adaptable to other watersheds facing similar pressures from LULC dynamics and supports policymakers in developing adaptive flood management strategies that integrate ecological perspectives into spatial planning.

Keywords-flood vulnerability; Krueng Baro watershed; land use and land cover; rainfall; river density

I. INTRODUCTION

A flood is a natural phenomenon caused by heavy rainfall that produces a large amount of runoff, raising the water level of rivers and increasing their flow. Floods expand floodplains by eroding natural embankments and inundating surrounding areas [1]. Flood is a dynamic process resulting from the complex interaction between river basin management and hydrometeorological, hydrogeological, and geomorphological conditions [2]. The causes of floods in Indonesia are influenced by five factors: rainfall, river sedimentation, errors in river channel planning and development, errors in land use planning and infrastructure development, and the destruction of watershed retention [3]. Recent studies on GIS-based flood vulnerability assessment commonly use multi-criteria scoring and weighting to integrate key biophysical and land-surface factors into a single vulnerability index [4, 5]. However, many studies provide limited discussion of how vulnerability patterns may change under different parameter selections within the

same workflow. To address the problem, this study implements multiple parameter scenarios within a consistent GIS-based hierarchical criteria analysis. It compares the resulting vulnerability patterns to identify the dominant drivers for better planning prioritization.

River floods caused by excessive rainfall runoff repeatedly damage river basins, where land surface characteristics have changed due to deforestation and urban growth. Decreased river network connectivity, loss of fluvial floodplains, and conversion of agricultural land to impermeable urban surfaces can significantly reduce the watershed's storm response time, thereby increasing peak flow and flood risk [6, 7]. Given these conditions, spatial analysis becomes increasingly important for understanding how physical and human-driven factors interact to shape flood vulnerability. Recent studies have shown that combining GIS with multi-criteria decision analysis can produce clear and reliable flood vulnerability maps, providing stronger support for planning and mitigation decisions [8]. LULC is closely linked to human activities and land resources [9]. Changes in land use that occur without planning and control will cause environmental damage [10], including reductions in ecosystem services, carbon stocks, and local climate change [11]. LULC change can introduce physical factors that drive flooding [12], thereby altering the frequency or likelihood of flooding. Soil, topography, and land-use changes are interrelated, and rainfall, runoff, and erosion rates are determined by the watershed parameters mentioned above [13]. Significant changes in LULC have drastically increased the number of floods. Changes in LULC can also alter the pattern and intensity of exposure, which are determined by land use. Recent research has shown that urban development and deforestation affect land use in many parts of the world. Deforested land and impermeable surfaces (buildings and roads) reduce infiltration, increase runoff, and shorten peak flood times in low-lying areas [14]. This study aims to contribute by (i) applying a GIS-based hierarchical scoring–weighting workflow across multiple parameter scenarios, (ii) identifying the dominant flood-related factors from comparative scenario results, and (iii) interpreting the mapped vulnerability in terms of spatial planning relevance at the watershed scale.

II. MATERIALS AND METHODS

A. Study Location

This study was conducted in the Krueng Baro Watershed (KBW) (Figure 1). This area is characterized by upstream–downstream elevation gradients and recurring flood exposure in downstream zones during periods of high rainfall. These physiographic conditions make the Krueng Baro Watershed suitable for analyzing vulnerability patterns derived from terrain, hydrologic, soil, and land-surface factors. This research method begins by collecting data from rainfall, soil type, slope, river density, LULC, and elevation maps. The data is obtained from the Regional Development Planning Agency of Pidie Regency. Using ArcGIS 10.8, the following steps are used to create flood-prone area distribution maps in the KBW using six, four, and three parameters.

B. Scoring

Each parameter (rainfall, land use, soil type, slope, elevation, and river density) was scored separately in ArcGIS, and the resulting scores are shown in Tables I–VI. Rainfall is strongly linked to surface runoff and erosion, with higher rainfall leading to greater runoff and erosion (Table I), thereby increasing flood potential in a watershed [15]. Rainfall data are also essential for water resource management and hydrological–ecological modeling, but records are often incomplete due to missing measurements or a limited number of rain-gauge stations in the study area [16].

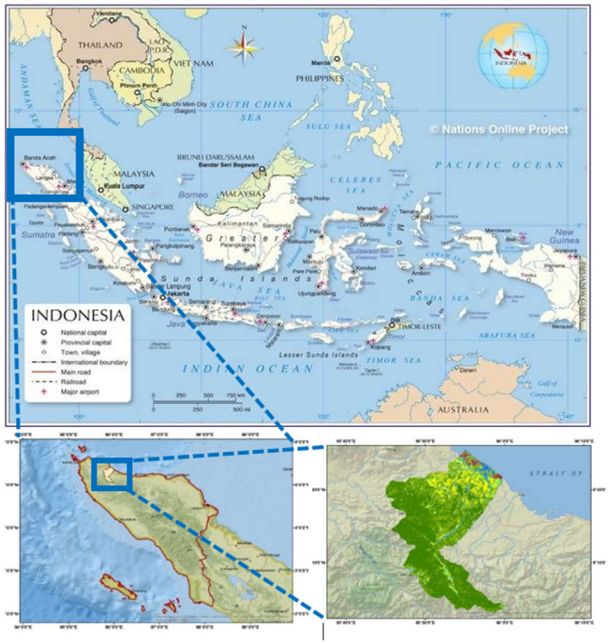

Fig. 1. Study location

TABLE I. RAINFALL SCORING

Rainfall (mm/year)	Score
>2500	9
2001-2500	7
1501-2000	5
1000-1500	3
<1000	1

Land use significantly affects a region's flood susceptibility, influencing the runoff generated when rainfall exceeds the infiltration rate. Land covered with dense vegetation allows for greater infiltration of rainwater. It increases the time runoff takes to reach the river, reducing the likelihood of flooding compared to areas without vegetation. Land use refers to human intervention in the land to meet livelihood needs (Table II). Agricultural land use is categorized based on water supply, the commodities produced, and the vegetation or crops on the land. In addition to climate, factors that influence flooding include soil type, land use, and an area's topography [17]. Based on these factors, various land uses include dryland farming (non-irrigated land), paddy fields, protected forests, production forests, coffee plantations, rubber plantations, grasslands, and savannahs.

TABLE II. LULC SCORING

LULC	Score
Open land – water body	9
Settlement – rice field	7
Plantation - gardens	5
Mixed plantation - shrubs	3
Forest	1

Soil infiltration refers to the soil's ability to allow water to move into and through its profile (Table III). This process enables the soil to temporarily store water (soil moisture), making it available for plants and soil organisms to uptake. When less water is stored in the soil for plant growth, crop production decreases, leading to reduced organic matter and weakened soil structure and texture.

TABLE III. SOIL TYPE SCORING

Soil type	Score
Vertisol, oxisol	9
Alfisol, ultisol, molisol	7
Inceptisol	5
Entisol, histosol	3
Spodosol, andisol	1

The permeability of a soil mass is closely related to its infiltration capacity, as infiltration is the process by which water enters the soil from the surface. Due to their distinct characteristics, different types of soil exhibit varying infiltration and percolation rates. Soil infiltration capacity refers to the maximum infiltration rate permitted by the soil's surface condition and top layer. In contrast, percolation capacity is the maximum percolation rate from the soil surface to the groundwater table under unsaturated conditions. Slope, or land gradient, is the percentage ratio of the vertical distance (land height) to the horizontal distance (flat land length). The gentler the slope, the higher the potential for flooding, and vice versa (Table IV).

TABLE IV. SLOPE SCORING

Slope (%)	Score
0-8	9
8-15	7
15-25	5
25-40	3
>40	1

The slope, a key topographical feature, greatly impacts surface runoff and erosion. Steeper slopes lead to higher surface runoff and greater force of movement. Additionally, slope length influences water flow on the soil surface; more water tends to flow, and its velocity tends to be higher at the slope's base than at the top (Table V).

TABLE V. RIVER DENSITY SCORING

River density (km/km^2)	Score
<0.25	7
0.25-10	5
10-25	3
>25	1

River density refers to the length of river flow per square kilometer of the watershed area. A higher river density value (Dd) indicates a better drainage system in the area. It means there is more total surface runoff (less infiltration) and less groundwater storage in that region [18]. River density is the ratio of the total river length (in km) to the watershed area [19]. It can be calculated using the formula [20]:

$$\mathrm{Dd} = Ln/A \quad (1)$$

where: Dd = river density (km/km^2); Ln = main river length (km); A = watershed area (km^2).

Land elevation is the height of a location above sea level (Table VI). Elevation significantly influences flood occurrence. The lower an area is, the higher its flood potential, and vice versa. Higher elevations are generally safer from flooding. Elevation is the vertical position of an area relative to a specific reference point, typically above sea level. It affects the flooding potential because water naturally flows from higher to lower elevations. Lower-lying areas are more prone to flooding, whereas higher regions are less likely to experience such events. Thus, regions at higher elevations tend to be less vulnerable to flooding than lowland areas.

TABLE VI. ELEVATION SCORE

Elevation (m)	Score
0-20	9
21-50	7
51-100	5
101-300	3
>300	1

C. Equations

After obtaining each parameter's score, the scores are weighted based on the number of parameters used. The weighting for the six parameters is shown in Tables VII-X. Each parameter layer was reclassified into ordinal scores using predetermined flood-relevance criteria. The weights represent each parameter's relative influence and are normalized so that the total weight is 1 (100%) in each scenario. The flood vulnerability index was computed as a weighted linear combination of the normalized scores. This procedure ensures comparability between scenarios while maintaining the same computational structure.

TABLE VII. WEIGHTING FOR SIX PARAMETERS

Parameter	Weight (%)
Rainfall	2.0
Slope	1.0
Soil type	1.0
Land use	2.5
Elevation	1.5
River density	2.0
Total	10.00

$$\text{Flood vulnerability} = (2 \text{ x Rainfall}) + (2.5 \text{ x Land Use}) + (1 \text{ x Slope}) + (1.5 \text{ x Elevation}) + (1 \text{ x Soil Type}) + (2 \text{ x River Density}) \quad (2)$$

TABLE VIII. WEIGHTING FOR FOUR PARAMETERS

Parameter	Weight (%)
Rainfall	3.0
Land use	3.5
Slope	1.5
Soil type	2.0
Total	10.0

$$\text{Flood vulnerability} = (3 \times \text{Rainfall}) + (3.5 \times \text{Land use}) + (1.5 \times \text{Slope steepness}) + (2 \times \text{Soil type}) \quad (3)$$

TABLE IX. WEIGHTING FOR THREE PARAMETERS

Parameter	Weight (%)
Rainfall	4.0
Slope	2.5
Soil type	3.5
Total	10.0

$$\text{Flood vulnerability} = (4 \times \text{Rainfall}) + (2.5 \times \text{Slope steepness}) + (3.5 \times \text{Soil type}) \quad (4)$$

The 3-parameter scenario (rainfall–slope–soil type) was designed as a biophysical basis for sensitivity comparisons; LULC was intentionally excluded from this basis and included only in the extended scenarios to represent anthropogenic surface modification. After obtaining the multiplication score and weight for each parameter, they are grouped according to the following flood vulnerability classification (Table X):

TABLE X. CLASSIFICATION OF FLOOD VULNERABILITY

Classification	Flood vulnerability score
Very low	0-20
Low	21-40
Moderate	41-60
High	61-80
Very high	81-100

The flood vulnerability maps are derived from various parameter scenarios, providing a clear spatial representation of vulnerability distribution across the watershed. These outputs enable a tangible comparison of vulnerability patterns and support the interpretation of the dominant flood-related drivers, prior to a detailed discussion of the results.

III. RESULTS

The mapping approach provides information on flood-prone areas [14]. Recent GIS-based flood vulnerability studies commonly use multi-criteria and hierarchical weighting approaches within GIS to integrate diverse flood-related factors [4, 5]. However, fewer studies examine how vulnerability patterns change under different parameter configurations within a consistent workflow. This study addresses that gap by comparing multiple parameter scenarios and clarifying the relative influence of key drivers on vulnerability distribution, providing practical insight for watershed-scale spatial planning and flood risk management. This information is important for shaping regional spatial plans for the Sigli urban area and its surroundings to reduce flood damage. Using six parameters (rainfall, soil type, slope gradient, river density, land use, and elevation), flood vulnerability in the KBW is classified into three classes: low (19,283.80 ha), medium (19,582.64 ha), and high (18,344.11 ha) (Figure 2).

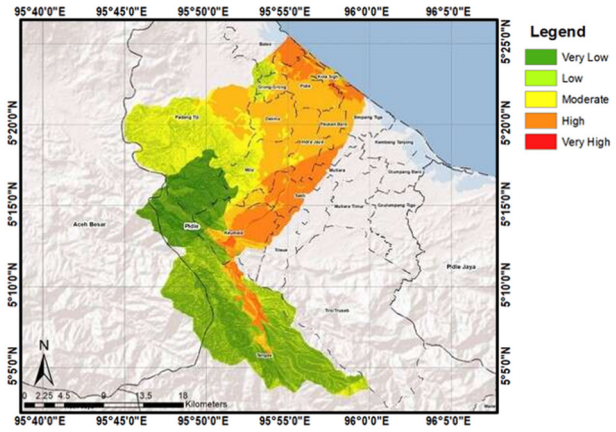

Fig. 2. Flood vulnerability with six parameters

This flood vulnerability map reflects the combined spatial influence of all contributing parameters within the applied modeling framework, particularly land use and elevation, which together shape the overall vulnerability pattern across the study area. Using four parameters (rainfall, soil type, slope, and land use), the KBW is also divided into three classes: low (6,276.91 ha), medium (29,716.73 ha), and high (21,216.91 ha) (Figure 3). Areas with moderate to high vulnerability may be more exposed due to limited flood-control infrastructure. At the same time, localized flooding is often linked to unplanned settlements that block drainage, inadequate drainage systems, and reduced capacity due to waterlogging [21]. A higher drainage density further increases the likelihood of flooding [6].

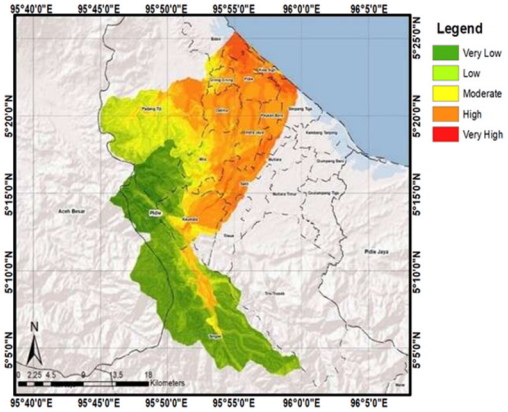

Fig. 3. Flood vulnerability with four parameters

The growth of urban areas near riverbanks has dramatically increased the probability, severity, and frequency of floods, making them among the most common and destructive natural disaster threats. Urbanization is expanding at the expense of

agricultural land, as areas designated for urban growth often fail to meet the growing population's demands. Additionally, these land-use shifts, driven by urban development, exacerbate the risk of flooding [8]. Tangse and Padang Tiji record the largest moderate-vulnerability areas at 12,254.59 ha and 9,544.98 ha, respectively, while Tiro/Truseb and Titeue contribute much smaller areas, indicating relatively limited overall vulnerability. Keumala stands out with a sizable, very high-vulnerability area of 2,692.34 ha, suggesting strong flood exposure likely influenced by topography, proximity to rivers, and land use patterns. Batee and Kota Sigli have only small areas in the very high vulnerability class, indicating local geographic and environmental differences. Moderate vulnerability is widespread, with Indra Jaya and Mila each exceeding 2,000 ha. Overall, Tangse has the largest total vulnerable area (16,291.50 ha), driven mainly by extensive low- and moderate-vulnerability zones.

Three parameters used to determine flood vulnerability are rainfall, soil type, and slope. The results of mapping flood vulnerability using these three parameters show that the KBW's flood vulnerability is divided into four classes: low class covering an area of 1.85, medium class covering an area of 39,070.72 ha, high class covering an area of 18,121.26 ha, and very high class covering an area of 16.72 ha (Figure 4).

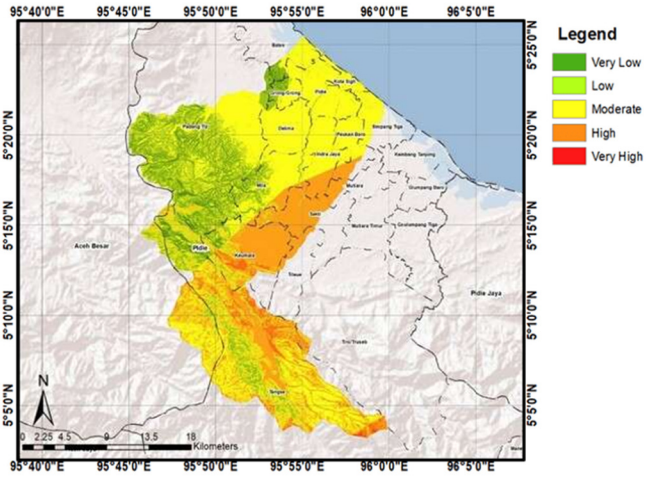

Fig. 4. Flood vulnerability with three parameters

Flood vulnerability based on these three parameters shows a very high flood vulnerability class covering an area of 16.72 ha, specifically in the Tangse sub-district (16.13 ha) and the Tiro/Truseb sub-district (0.59 ha). Flood vulnerability using these three parameters does not include land use. Figure 4 presents flood vulnerability across districts in Aceh and Pidie regencies, classified into five levels (very low to very high) based on affected area (ha). The observed variations are likely driven by differences in topography, rainfall patterns, land use, and population density. In Aceh Jaya Regency, vulnerability is relatively high, with the low (1,717.95 ha) and high (1,537.11 ha) classes dominating, for a total vulnerable area of 3,255.06 ha, indicating higher exposure than in several districts in Pidie Regency. In Pidie Regency, flood vulnerability varies across districts. Padang Tiji has the largest low-vulnerability area at 13,724.43 ha and a total vulnerable area of 13,854.82 ha. By comparison, Tangse has extensive moderate (7,626.04 ha) and high (8,648.70 ha) areas, making it the most affected overall (16,291.50 ha). Keumala also records a sizeable moderate-vulnerability area (3,396.63 ha), indicating localized flooding. These patterns likely reflect local conditions, such as proximity to river basins and high rainfall, whereas Delima and Mila show lower vulnerability due to lower exposure or better flood management.

IV. DISCUSSION

To meet the increasing demands of life, humans are engaging in large-scale resource exploitation within the watershed. Uncontrolled exploitation of watershed resources leads to declines in the watershed's physical and environmental conditions. One indicator of deteriorating watershed conditions is landscape change caused by land-use conversion. One way to increase plantation production is through agricultural extensification efforts. The problem is the increasing surface flow from LULC conversion, which is affecting the watershed outlet's peak discharge. LULC conversion also hardens soil due to human intervention, reducing its infiltration capacity. If no further management is implemented, peak discharge will increase each year, potentially causing flooding in the middle and downstream areas.

LULC patterns, in various forms and methods, will affect the environment [22]. A decline in environmental carrying capacity in a region can be seen in various disasters, such as floods, and the continuous decrease in forest area increases the likelihood of floods [23, 24]. The presence of forests can support other efforts to reduce flood frequency [25]. In addition, forests maintain the continuity of water flow by regulating it: they store water during the rainy season and release it during the dry season. The change in LULC due to urban development is inevitable, beginning with deforestation and progressing to impermeable surfaces such as house roofs. This change has increased the frequency and intensity of floods. LULC is the only factor that affects the watershed's response, particularly peak flood discharge [26]. LULC change, or land-use shift, is the transition of land from one use to another. LULC changes from non-built-up areas, such as fields or yards, to built-up areas, including residential areas, offices, or industrial areas, will reduce the land's ability to absorb rainwater [27].

Other studies focus on LULC and its impact on flooding in the Maros River Basin Area [28]. The data consisted of time-series data on flood areas and changes in built-up areas from 2015 to 2019, which were entered into SPSS 22.0 and analyzed using linear regression with the enter method. The results showed that the increasing use of built-up areas directly led to sealing relatively impermeable land surfaces (land concretization). The reduction in water infiltration from built-up areas, on the other hand, would increase surface runoff, thereby increasing the likelihood of flooding.

Uncontrolled urban and regional spatial development due to urbanization has led to an increasing trend in flooding issues. Within urban spatial development, activities to meet human

needs will increase across economic, social, and environmental dimensions. As a result, there is excessive exploitation of nature, uncontrolled LULC changes, and a decrease in environmental sustainability [25, 29]. Conducting analyses and mapping flood hazards is essential for anticipating and reducing the impact of future flood events. This approach helps identify vulnerable areas based on physical characteristics that influence flood susceptibility. Flood hazard mapping plays a pivotal role in planning for flood-prone regions and developing effective mitigation strategies [30].

Urban growth and infrastructure are also linked to changes in hydrological and ecological systems, the loss of drainage systems, and increased vulnerability to flooding. In addition, infrastructure development, such as dense road construction, also affects urban flooding [31]. Flooding is a dynamic process driven by the complex interaction among river basin management and hydrometeorological, hydrogeological, and geomorphological conditions. It is a complex, nonlinear process that may never be effectively controlled by simple linear processes [4]. Flooding is associated with land cover change, population growth, and road density [28]. The results show that Moran's I index, which reflects spatial correlation, indicates that the values for three pairs (RCF-LC, RCF-PG, and RCF-RD) are positive and close to 0. These results indicate that these pairs exhibit a clustered, significant distribution, suitable for examining spatial correlation. In addition, the critical value obtained (z) exceeds 2.58, indicating a probability of <1% that clustering patterns will occur randomly. Therefore, relative changes in flood areas can be related to land use, population growth, and road network expansion.

Land slope influences surface flow velocity and can increase peak river discharge. Gentle slopes of 0–8% are often flood-prone because water accumulates in lower areas [32]. Elevation is also critical, as floods tend to occur more frequently in low-lying terrain, although relevant elevation thresholds vary by local topography, flood dynamics, and study scope [33]. In addition, vulnerability is shaped by drainage conditions and proximity to drainage networks, as well as by slope-driven runoff and LULC patterns, which strongly influence flood exposure [34]. The LULC pattern strongly influences rainfall-induced runoff, thereby affecting the likelihood of flooding [7]. LULC affects water distribution through the infiltration balance [33, 34]. Therefore, mapping flood areas is needed to support policies, as areas prone to flooding will affect the community, including damage to agricultural land, reduced asset values, and a weakened economy. This flood vulnerability map provides a practical basis for spatial planning to prioritize flood-risk mitigation in high-vulnerability zones within the watershed.

V. CONCLUSION

The difference in the number of parameters used to determine flood-prone areas depends on the conditions in the KBW. Determination of flood areas without considering land use, using three parameters (rainfall, soil, and slope), yields a high-flood classification area of 18,137.98 ha and a medium classification area of 39,070.72 ha. Using four parameters plus land use, the area of highly vulnerable flood-prone areas is 21,216.91 ha, and the medium area is 29,716.73 ha. When adding drainage density and elevation, the area of very high flood-prone areas increases to 18,344.11 ha, while the medium flood-vulnerability area increases to 19,582.64 ha. It means that river density, elevation, and land use also determine flood-prone areas. Therefore, river normalization and land use protection can reduce the occurrence of additional flood areas.

ACKNOWLEDGMENT

The authors wish to thank Universitas Syiah Kuala and the Ministry of Education, Culture, Research, and Technology, Republic of Indonesia, for their support of this research. Contract No. 652/UN11.2.1/PT.01.03/DPRM/2023.

REFERENCE

[1] A. Haghizadeh, S. Siahkamari, A. H. Haghiabi, and O. Rahmati, "Forecasting flood-prone areas using Shannon's entropy model," *Journal of Earth System Science*, vol. 126, no. 3, Mar. 2017, Art. no. 39, https://doi.org/10.1007/s12040-017-0819-x.

[2] K. Khosravi *et al.*, "Convolutional neural network approach for spatial prediction of flood hazard at national scale of Iran," *Journal of Hydrology*, vol. 591, Dec. 2020, Art. no. 125552, https://doi.org/10.1016/j.jhydrol.2020.125552.

[3] O. S. Areu-Rangel, L. Cea, R. Bonasia, and V. J. Espinosa-Echavarria, "Impact of Urban Growth and Changes in Land Use on River Flood Hazard in Villahermosa, Tabasco (Mexico)," *Water*, vol. 11, no. 2, Feb. 2019, Art. no. 304, https://doi.org/10.3390/w11020304.

[4] D. Nsangou *et al.*, "Urban flood susceptibility modelling using AHP and GIS approach: case of the Mfoundi watershed at Yaoundé in the South-Cameroon plateau," *Scientific African*, vol. 15, Mar. 2022, Art. no. e01043, https://doi.org/10.1016/j.sciaf.2021.e01043.

[5] R. Mann and A. Gupta, "Mapping flood vulnerability using an analytical hierarchy process (AHP) in the Metropolis of Mumbai," *Environmental Monitoring and Assessment*, vol. 195, no. 12, Nov. 2023, Art. no. 1534, https://doi.org/10.1007/s10661-023-12141-5.

[6] F. L. Ogden, N. Raj Pradhan, C. W. Downer, and J. A. Zahner, "Relative importance of impervious area, drainage density, width function, and subsurface storm drainage on flood runoff from an urbanized catchment," *Water Resources Research*, vol. 47, no. 12, 2011, https://doi.org/10.1029/2011WR010550.

[7] M. Szwagrzyk, D. Kaim, B. Price, A. Wypych, E. Grabska, and J. Kozak, "Impact of forecasted land use changes on flood risk in the Polish Carpathians," *Natural Hazards*, vol. 94, no. 1, pp. 227–240, Oct. 2018, https://doi.org/10.1007/s11069-018-3384-y.

[8] K. Loumi and A. Redjem, "Integration of GIS and Hierarchical Multi-Criteria Analysis for Mapping Flood Vulnerability: The Case Study of M'sila, Algeria," *Engineering, Technology & Applied Science Research*, vol. 11, no. 4, pp. 7381–7385, Aug. 2021, https://doi.org/10.48084/etasr.4266.

[9] S. R. P. Sitorus, B. Susanto, and O. Haridjaja, "A Preliminary Criteria and Classification of Land Degradation Level on Dryland (Case Study : Dryland in Bogor Regency)," *Indonesian Soil and Climate Journal*, no. 34, pp. 48–65, 2011, https://doi.org/10.2017/jti.v0n34.2011.48-65.

[10] W. Masyhuri, "Analisa perubahan penggunaan lahan terhadap potensi banjir di Medan Denai (Analysis of Land Use Change on Flood Potential in Medan Denai)," *Tunas Geografi*, vol. 7, no. 2, pp. 127–132, 2018, https://doi.org/10.24114/tgeo.v7i1.7192.

[11] I. Ramli, A. Achmad, and A. Anhar, "Temporal changes in Land Use and Land Cover (LULC) and local climate in the Krueng Peusangan Watershed (KPW) area, Aceh, Indonesia," *Bulletin of Geography. Socio-economic Series*, no. 59, pp. 161–165, Mar. 2023, https://doi.org/10.12775/bgss-2023-0010.

[12] A. M. Caldas *et al.*, "Flood Vulnerability, Environmental Land Use Conflicts, and Conservation of Soil and Water: A Study in the Batatais SP Municipality, Brazil," *Water*, vol. 10, no. 10, Sept. 2018, Art. no. 1357, https://doi.org/10.3390/w10101357.

[13] B. Saghafian, H. Farazjoo, B. Bozorgy, and F. Yazdandoost, "Flood Intensification due to Changes in Land Use," *Water Resources Management*, vol. 22, no. 8, pp. 1051–1067, Aug. 2008, https://doi.org/10.1007/s11269-007-9210-z.

[14] S. Janizadeh *et al.*, "Mapping the spatial and temporal variability of flood hazard affected by climate and land-use changes in the future," *Journal of Environmental Management*, vol. 298, Nov. 2021, Art. no. 113551, https://doi.org/10.1016/j.jenvman.2021.113551.

[15] A. Phinyoyang and S. Ongsomwang, "Optimizing Land Use and Land Cover Allocation for Flood Mitigation Using Land Use Change and Hydrological Models with Goal Programming, Chaiyaphum, Thailand," *Land*, vol. 10, no. 12, Nov. 2021, Art. no. 1317, https://doi.org/10.3390/land10121317.

[16] X. Yang, X. Xie, D. L. Liu, F. Ji, and L. Wang, "Spatial Interpolation of Daily Rainfall Data for Local Climate Impact Assessment over Greater Sydney Region," *Advances in Meteorology*, vol. 2015, no. 1, 2015, Art. no. 563629, https://doi.org/10.1155/2015/563629.

[17] R. Rahmi, A. Ahmad, A. Yulianur, I. Ramli, and A. Izzaty, "Spatial Analysis of Flood Vulnerability Base on Biophysics Factor the Krueng Baro Watershed in Flood Mitigation Efforts at Aceh, Indonesia," *BIO Web of Conferences*, vol. 96, 2024, Art. no. 04002, https://doi.org/10.1051/bioconf/20249604002.

[18] J. P. Matondang, S. Kahar, and B. Sasmito, "Analisis Zonasi Daerah Rentan Banjir Dengan Pemanfaatan Sistem Informasi Geografis (Studi Kasus : Kota Kendal Dan Sekitarnya)(Flood-Prone Area Zoning Analysis Using Geographic Information Systems (Case Study: Kendal City and Surrounding Areas)," *Jurnal Geodesi Undip*, vol. 2, no. 2, pp. 103–113, Apr. 2013.

[19] H. Harisagustinawati, A. Aswandi, and S. Sunarti, "Karakter DAS Kambang Berdasarkan Analisis Morfometri dan Aspek Biofisik," *Jurnal Daur Lingkungan*, vol. 3, no. 2, pp. 38–41, Aug. 2020, https://doi.org/10.33087/daurling.v3i2.51.

[20] E. S. Ningkeula, "Analisis karakteristik morfometri dan hidrologi sebagai ciri karakteristik biogeofisik DAS Wai Samal Kecamatan Seram Utara Timur Kobi Kabupaten Maluku Tengah ((Analysis of Morphometric and Hydrological Characteristics as Biogeophysical Features of the Wai)," *Agrikan: Jurnal Agribisnis Perikanan*, vol. 9, no. 2, pp. 76–86, Oct. 2016, https://doi.org/10.29239/j.agrikan.9.2.76-86.

[21] P. T. Kadave, A. D. Kale, and S. Narwade, "Mumbai Floods, Reasons and Solutions," *International Journal of Scientific and Research Publications*, vol. 6, no. 3, pp. 224–228, Mar. 2016.

[22] J. A. Foley *et al.*, "Global Consequences of Land Use," *Science*, vol. 309, no. 5734, pp. 570–574, July 2005, https://doi.org/10.1126/science.1111772.

[23] Q. Rong, Y. Cai, M. Su, W. Yue, Z. Dang, and Z. Yang, "Identification of the optimal agricultural structure and population size in a reservoir watershed based on the water ecological carrying capacity under uncertainty," *Journal of Cleaner Production*, vol. 234, pp. 340–352, Oct. 2019, doi: 10.1016/j.jclepro.2019.06.179.

[24] Y. Wang, Y. Wang, X. Su, L. Qi, and M. Liu, "Evaluation of the comprehensive carrying capacity of interprovincial water resources in China and the spatial effect," *Journal of Hydrology*, vol. 575, pp. 794–809, Aug. 2019, https://doi.org/10.1016/j.jhydrol.2019.05.076.

[25] C. Asdak, *Hidrologi dan Pengelolaan Daerah Aliran Sungai*, revised ed. Yogyakarta, Indonesia: Gadjah Mada University Press, 2022.

[26] E. H. Nurrizqi and S. Suyono, "Pengaruh Perubahan Penggunaan Lahan Terhadap Perubahan Debit Puncak Banjir Di Sub Das Brantas Hulu," *Jurnal Bumi Indonesia*, vol. 1, no. 3, pp. 363–371, 2012.

[27] B. Surya *et al.*, "Spatial Transformation of a New City in 2006–2020: Perspectives on the Spatial Dynamics, Environmental Quality Degradation, and Socio—Economic Sustainability of Local Communities in Makassar City, Indonesia," *Land*, vol. 9, no. 9, Sept. 2020, Art. no. 324, https://doi.org/10.3390/land9090324.

[28] R. Latief, R. A. Barkey, and Muh. I. Suhaeb, "Perubahan Penggunaan Lahan Terhadap Banjir di Kawasan Daerah Aliran Sungai Maros," *Urban and Regional Studies Journal*, vol. 3, no. 2, pp. 52–59, June 2021, https://doi.org/10.35965/ursj.v3i2.669.

[29] D. Hermon, "Estimate of Changes in Carbon Stocks Based on Land Cover Changes in the Leuser Ecosystem Area (LEA) Indonesia," *Forum Geografi*, vol. 29, no. 2, pp. 188–196, Feb. 2016, https://doi.org/10.23917/forgeo.v29i2.1487.

[30] G. D. Bhatt, K. Sinha, P. K. Deka, and A. Kumar, "Flood Hazard and Risk Assessment in Chamoli District, Uttarakhand Using Satellite Remote Sensing and GIS Techniques," *International Journal of Innovative Research in Science, Engineering and Technology*, vol. 03, no. 08, pp. 15348–15356, Aug. 2014, https://doi.org/10.15680/IJIRSET.2014.0308039.

[31] J. Yin, D. Yu, Z. Yin, M. Liu, and Q. He, "Evaluating the impact and risk of pluvial flash flood on intra-urban road network: A case study in the city center of Shanghai, China," *Journal of Hydrology*, vol. 537, pp. 138–145, June 2016, https://doi.org/10.1016/j.jhydrol.2016.03.037.

[32] M. S. G. Adnan, A. Y. M. Abdullah, A. Dewan, and J. W. Hall, "The effects of changing land use and flood hazard on poverty in coastal Bangladesh," *Land Use Policy*, vol. 99, Dec. 2020, Art. no. 104868, https://doi.org/10.1016/j.landusepol.2020.104868.

[33] I. Ramli, S. Murthada, Z. Nasution, and A. Achmad, "Hydrograph separation method and baseflow separation using Chapman Method – A case study in Peusangan Watershed," *IOP Conference Series: Earth and Environmental Science*, vol. 314, no. 1, Dec. 2019, Art. no. 012026, https://doi.org/10.1088/1755-1315/314/1/012026.

[34] X. Li, Y. Zhang, N. Ma, C. Li, and J. Luan, "Contrasting effects of climate and LULC change on blue water resources at varying temporal and spatial scales," *Science of The Total Environment*, vol. 786, Sept. 2021, Art. no. 147488, https://doi.org/10.1016/j.scitotenv.2021.147488.